EARTHQUAKE ENGINEERING AND STRUCTURAL DYNAMICS
Earthquake Engng Struct. Dyn. 2003; **32**:751–770 (DOI: 10.1002/eqe.247)

Reliability-based robust control for uncertain dynamical systems using feedback of incomplete noisy response measurements

Ka-Veng Yuen and James L. Beck*,†

Division of Engineering and Applied Science, California Institute of Technology, 1201 E. California Blvd, Pasadena, CA 91125, U.S.A.

SUMMARY

A reliability-based output feedback control methodology is presented for controlling the dynamic response of systems that are represented by linear state-space models. The design criterion is based on a robust failure probability for the system. This criterion provides robustness for the controlled system by considering a probability distribution over a set of possible system models with a stochastic model of the excitation so that robust performance is expected. The control command signal can be calculated using incomplete response measurements at previous time steps without requiring state estimation. Examples of robust structural control using an active mass driver on a shear building model and on a benchmark structure are presented to illustrate the proposed method. Copyright © 2003 John Wiley & Sons, Ltd.

KEY WORDS: benchmark control problem; robust control; robust failure probability; robust reliability; stochastic control; structural control

1. INTRODUCTION

Because complete information about a dynamical system and its environment are never available, the system and excitation cannot be modelled exactly. Classical control design methods based on a single nominal model of the system may fail to create a control system that provides satisfactory performance. Robust control methods (e.g. $\mathscr{H}_2$, $\mathscr{H}_\infty$ and μ-synthesis, etc.) were therefore proposed so that the optimal controller can provide robust performance and stability for a set of 'possible' models of the system [1, 2]. In a probabilistic robust control approach, an additional 'dimension' is introduced by using probabilistic descriptions of all the possible models when selecting the controller to achieve optimal performance. These probability distributions give a measure of how plausible the possible parameter values are, and

* Correspondence to: James L. Beck, Division of Engineering and Applied Science, California Institute of Technology, 1201 E. California Blvd, Pasadena, CA 91125, U.S.A.
† E-mail: jimbeck@cco.caltech.edu

Received 5 December 2001
Revised 6 August 2002
Accepted 13 August 2002

they may be obtained from engineering judgement or Bayesian system identification methods [3–5].

Over the last decade or so, there has been increasing interest in probabilistic, or stochastic, robust control theory. Monte Carlo simulations methods have been used to synthesize and analyze controllers for uncertain systems [6, 7]. In References [8–11], first- and second-order reliability methods were incorporated to compute the probable performance of linear-quadratic-regulator controllers (LQR). On the other hand, an efficient asymptotic expansion [12] was used to approximate the probability integrals that are needed to determine the optimal parameters for a passive tuned mass damper [13] and the optimal gains for an active mass driver [14] for robust structural control. In Reference [14], the proposed controller feeds back output measurements at the current time only, where the output corresponds to certain response quantities that need not be the full state vector of the system. However, there is additional information from past output measurements which may improve the performance of the control system.

In this paper, the reliability-based methodology proposed in Reference [14] is extended to allow feedback of the output (partial state) measurements at previous time steps. It is noted that in traditional linear-quadratic-Gaussian (LQG) control with partial state measurements, the optimal controller can be achieved by estimating the full state using a Kalman filter combined with the optimal LQG controller for full state feedback. However, in our case the separation principle does not apply and no state estimation is needed. The method presented for reliability-based robust control design may be applied to any system represented by linear state-space models but the focus here is on robust control of structures [15–17].

In Section 2, an augmented vector formulation is presented for treating the output history feedback. Then, the statistical properties of the response quantities are calculated using the Lyapunov equation in discrete form. In Section 3, the robust control method is introduced which is based on choosing the feedback gains to minimize the robust failure probability [18]. In Section 4, examples using a shear building model and a benchmark structure are given to illustrate the proposed approach.

2. STOCHASTIC RESPONSE ANALYSIS FOR CONTROLLER DESIGN

For the purpose of designing a controller for a structure and control system, a model of the structural behavior must first be formulated. Suppose it is a linear model with N_d degrees-of-freedom (DOFs) and equation of motion

$$\mathbf{M}(\boldsymbol{\theta}_s)\ddot{\mathbf{x}}(t) + \mathbf{C}(\boldsymbol{\theta}_s)\dot{\mathbf{x}}(t) + \mathbf{K}(\boldsymbol{\theta}_s)\mathbf{x}(t) = \mathbf{T}\cdot\mathbf{f}(t) + \mathbf{T}_c\cdot\mathbf{f}_c(t) \tag{1}$$

where $\mathbf{M}(\boldsymbol{\theta}_s)$, $\mathbf{C}(\boldsymbol{\theta}_s)$ and $\mathbf{K}(\boldsymbol{\theta}_s)$ are the $N_d \times N_d$ mass, damping and stiffness matrix, respectively, parameterized by the structural parameters $\boldsymbol{\theta}_s$ of the system; $\mathbf{f}(t) \in \mathbb{R}^{N_f}$ and $\mathbf{f}_c(t) \in \mathbb{R}^{N_{fc}}$ are the external excitation and control force vector, respectively, and $\mathbf{T} \in \mathbb{R}^{N_d \times N_f}$ and $\mathbf{T}_c \in \mathbb{R}^{N_d \times N_{fc}}$ are their distribution matrices. A control law is to be chosen to determine $\mathbf{f}_c$ by feedback of the measured output.

The uncertain future excitation $\mathbf{f}(t)$ could be earthquake ground motions or wind forces, for example, and it is modelled by a zero-mean stationary filtered white-noise process described

by

$$\begin{aligned}\dot{\mathbf{w}}_f(t) &= \mathbf{A}_{\mathrm{w}f}(\boldsymbol{\theta}_f)\mathbf{w}_f(t) + \mathbf{B}_{\mathrm{w}f}(\boldsymbol{\theta}_f)\mathbf{w}(t)\\ \mathbf{f}(t) &= \mathbf{C}_{\mathrm{w}f}(\boldsymbol{\theta}_f)\mathbf{w}_f(t)\end{aligned} \tag{2}$$

where $\mathbf{w}(t) \in \mathbb{R}^{N_{\mathrm{w}}}$ is a Gaussian white-noise process with zero mean and unit spectral intensity matrix; $\mathbf{w}_f(t) \in \mathbb{R}^{N_{\mathrm{w}f}}$ is an internal filter state and $\mathbf{A}_{\mathrm{w}f}(\boldsymbol{\theta}_f) \in \mathbb{R}^{N_{\mathrm{w}f} \times N_{\mathrm{w}f}}$, $\mathbf{B}_{\mathrm{w}f}(\boldsymbol{\theta}_f) \in \mathbb{R}^{N_{\mathrm{w}f} \times N_{\mathrm{w}}}$ and $\mathbf{C}_{\mathrm{w}f}(\boldsymbol{\theta}_f) \in \mathbb{R}^{N_f \times N_{\mathrm{w}f}}$ are the parameterized filter matrices governing the properties of the filtered white noise. A vector $\boldsymbol{\theta}$ is introduced, which combines the structural parameter vector and the excitation parameter vector, i.e. $\boldsymbol{\theta} = [\boldsymbol{\theta}_s^{\mathrm{T}}, \boldsymbol{\theta}_f^{\mathrm{T}}]^{\mathrm{T}} \in \mathbb{R}^{N_s}$. The dependence on $\boldsymbol{\theta}$ will be left implicit hereafter in this section.

Denote the state vector as: $\mathbf{y}(t) = [\mathbf{x}(t)^{\mathrm{T}}, \dot{\mathbf{x}}(t)^{\mathrm{T}}]^{\mathrm{T}}$. Equation (1) can be rewritten in the state-space form as follows:

$$\dot{\mathbf{y}}(t) = \mathbf{A}_y\mathbf{y}(t) + \mathbf{B}_y\mathbf{f}(t) + \mathbf{B}_{y\mathrm{c}}\mathbf{f}_{\mathrm{c}}(t) \tag{3}$$

where $\mathbf{A}_y = \begin{bmatrix} \mathbf{0}_{N_{\mathrm{d}} \times N_{\mathrm{d}}} & \mathbf{I}_{N_{\mathrm{d}}} \\ -\mathbf{M}^{-1}\mathbf{K} & -\mathbf{M}^{-1}\mathbf{C} \end{bmatrix}$, $\mathbf{B}_y = \begin{bmatrix} \mathbf{0}_{N_{\mathrm{d}} \times N_f} \\ \mathbf{M}^{-1}\mathbf{T} \end{bmatrix}$ and $\mathbf{B}_{y\mathrm{c}} = \begin{bmatrix} \mathbf{0}_{N_{\mathrm{d}} \times N_{f\mathrm{c}}} \\ \mathbf{M}^{-1}\mathbf{T}_{\mathrm{c}} \end{bmatrix}$. Here, $\mathbf{0}_{a \times b}$ and $\mathbf{I}_a$ denote the $a \times b$ zero and $a \times a$ identity matrix, respectively.

In order to allow modelling of the sensor and actuator dynamics of the control system, and to allow more choices of the output to be fed back or to be controlled, an additional state vector $\mathbf{y}_f \in \mathbb{R}^{N_{yf}}$ is introduced whose dynamics are modelled by the following equation:

$$\dot{\mathbf{y}}_f(t) = \mathbf{A}_{yf}\mathbf{y}_f(t) + \mathbf{B}_{yf}\mathbf{y}(t) + \mathbf{B}_{y\mathrm{w}}\mathbf{w}_f(t) + \mathbf{B}_{yu}\mathbf{u}(t) \tag{4}$$

where $\mathbf{A}_{yf} \in \mathbb{R}^{N_{yf} \times N_{yf}}$, $\mathbf{B}_{yf} \in \mathbb{R}^{N_{yf} \times 2N_{\mathrm{d}}}$, $\mathbf{B}_{y\mathrm{w}} \in \mathbb{R}^{N_{yf} \times N_{\mathrm{w}f}}$, $\mathbf{B}_{yu} \in \mathbb{R}^{N_{yf} \times N_u}$ are the matrices that characterize the sensor and actuator dynamics and $\mathbf{u}(t) \in \mathbb{R}^{N_u}$ is the control command signal to be specified by a control law.

When Equation (4) is used to include a linear model of the actuator dynamics, the actuator forces are given by

$$\mathbf{f}_{\mathrm{c}}(t) = \mathbf{C}_{yf}\mathbf{y}_f(t) \tag{5}$$

For example, hydraulic actuators may be modelled using a first-order differential equation [19]:

$$\dot{f_{\mathrm{c}}} = A_f f_{\mathrm{c}} + B_f \dot{x}_a + B_{fu} u \tag{6}$$

where f_{c} is the control force applied by the actuator; $\dot{x}_a$ is the actuator velocity; u is the signal given to the actuator; and A_f, B_f and B_{fu} are given by

$$A_f = -\frac{2\beta k_a}{V}, \quad B_f = -\frac{2\beta A^2}{V}, \quad B_{fu} = \frac{2\beta A k_q}{V} \tag{7}$$

where β is the bulk modulus of the fluid; k_a and k_q are the controller constants; V is the characteristic hydraulic fluid volume of the actuator; and A is the cross-sectional area of the actuator. It is assumed here that the model for the actuator dynamics has been reliably

developed prior to its application for the structure. Another possibility is that the parameters involved in the actuator model are uncertain and so are included in the previously defined parameter vector $\boldsymbol{\theta}$.

The state vector $\mathbf{y}_f$ may also represent many choices of output. For example, it can handle displacement, velocity or acceleration measurements if the matrices in Equation (4) are chosen appropriately [20]. Accelerations can be obtained approximately by passing the velocities in the state vector $\mathbf{y}$ through a filter whose dynamics in Equation (4) represent the transfer function $H_{\mathrm{d}}(s) = \omega_0^2 s/(s^2 + \sqrt{2}\omega_0 s + \omega_0^2)$. This filter can approximate differentiation accurately if ω_0 is chosen larger than the upper limit of the frequency band of interest. On the other hand, Equation (4) also allows modelling of the sensor dynamics. For example, to model the limited bandwidth of a sensor, the dynamics in Equation (4) can represent a low-pass filter with the transfer function $H_l(s) = \omega_0^2/(s^2 + \sqrt{2}\omega_0 s + \omega_0^2)$.

If the full state vector $\mathbf{v}(t) = [\mathbf{w}_f(t)^{\mathrm{T}}, \mathbf{y}(t)^{\mathrm{T}}, \mathbf{y}_f(t)^{\mathrm{T}}]^{\mathrm{T}}$ is introduced, then Equations (2)–(4) can be combined as follows:

$$\dot{\mathbf{v}}(t) = \mathbf{A}\mathbf{v}(t) + \mathbf{B}\mathbf{w}(t) + \mathbf{B}_{\mathrm{c}}\mathbf{u}(t) \tag{8}$$

where the matrices $\mathbf{A}$, $\mathbf{B}$ and $\mathbf{B}_{\mathrm{c}}$ are given by

$$\mathbf{A} \equiv \begin{bmatrix} \mathbf{A}_{\mathrm{w}f} & \mathbf{0}_{N_{\mathrm{w}f}\times 2N_{\mathrm{d}}} & \mathbf{0}_{N_{\mathrm{w}f}\times N_{yf}} \\ \mathbf{B}_y\mathbf{C}_{\mathrm{w}f} & \mathbf{A}_y & \mathbf{B}_{y\mathrm{c}}\mathbf{C}_{yf} \\ \mathbf{B}_{y\mathrm{w}} & \mathbf{B}_{yf} & \mathbf{A}_{yf} \end{bmatrix}, \quad \mathbf{B} \equiv \begin{bmatrix} \mathbf{B}_{\mathrm{w}f} \\ \mathbf{0}_{2N_{\mathrm{d}}\times N_{\mathrm{w}}} \\ \mathbf{0}_{N_{yf}\times N_{\mathrm{w}}} \end{bmatrix} \quad \text{and} \quad \mathbf{B}_{\mathrm{c}} \equiv \begin{bmatrix} \mathbf{0}_{N_{\mathrm{w}f}\times N_u} \\ \mathbf{0}_{2N_{\mathrm{d}}\times N_u} \\ \mathbf{B}_{yu} \end{bmatrix} \tag{9}$$

By treating $\mathbf{w}$ and $\mathbf{u}$ as constant over each subinterval $[k\Delta t, k\Delta t + \Delta t)$, where Δt is the sampling time interval that is small enough to capture the dynamics of the structure, Equation (8) yields the following discrete-time equation:

$$\mathbf{v}[k+1] = \bar{\mathbf{A}}\mathbf{v}[k] + \bar{\mathbf{B}}\mathbf{w}[k] + \bar{\mathbf{B}}_{\mathrm{c}}\mathbf{u}[k] \tag{10}$$

where $\mathbf{v}[k] \equiv \mathbf{v}(k\Delta t)$, $\bar{\mathbf{A}} \equiv \mathrm{e}^{\mathbf{A}\Delta t}$, $\bar{\mathbf{B}} \equiv \mathbf{A}^{-1}(\bar{\mathbf{A}} - \mathbf{I}_{N_{\mathrm{w}f}+2N_{\mathrm{d}}+N_{yf}})\mathbf{B}$ and $\bar{\mathbf{B}}_{\mathrm{c}} \equiv \mathbf{A}^{-1}(\bar{\mathbf{A}} - \mathbf{I}_{N_{\mathrm{w}f}+2N_{\mathrm{d}}+N_{yf}})\mathbf{B}_{\mathrm{c}}$, $\mathbf{w}[k]$ is Gaussian discrete white noise with zero mean and covariance matrix $\boldsymbol{\Sigma}_{\mathrm{w}} = (2\pi/\Delta t)\mathbf{I}_{N_{\mathrm{w}}}$; and $\mathbf{u}[k]$ is given in terms of the measured output by specifying a control law.

Assume that discrete-time response data, with sampling time interval Δt, is available for N_o components of the output state, that is, the measured output is given by

$$\mathbf{z}[k] = \mathbf{L}_0\mathbf{v}[k] + \mathbf{n}[k] \tag{11}$$

where $\mathbf{L}_0 \in \mathbb{R}^{N_o \times (N_{\mathrm{w}f}+2N_{\mathrm{d}}+N_{yf})}$ is the observation matrix and $\mathbf{n}[k] \in \mathbb{R}^{N_o}$ is the uncertain prediction error which accounts for the difference between the actual measured output from the structural system and the predicted output given by the model defined by Equation (10); it includes both modelling error and measurement noise. The prediction error is modelled as a stationary Gaussian discrete white noise process with zero mean and covariance matrix $\boldsymbol{\Sigma}_{\boldsymbol{n}}$; this choice gives the maximum information entropy (greatest uncertainty) in the absence of any additional information about the unmodelled dynamics or output noise. Notice that $\mathbf{z}[k]$

is a linear combination of $\mathbf{w}_f[k]$, $\mathbf{y}[k]$ and $\mathbf{y}_f[k]$ and so it may include measured excitation, measured displacements, velocities and accelerations, and measured control forces.

Now, choose a linear control feedback law using the current and the previous N_p output measurements,

$$\mathbf{u}[k] = \sum_{p=0}^{N_p} \mathbf{G}_p \mathbf{z}[k - p] \tag{12}$$

where $\mathbf{G}_p,\ p = 0, 1, \ldots, N_p$ are the gain matrices, which will be determined in the next section. It is worth noting that if the matrices $\mathbf{G}_p,\ p = 0, \ldots, N_p^*(N_p^* < N_p)$ are fixed to be zero, the controller at any time step only uses output measurements from time steps that are more than $N_p^* \Delta t$ back in the past. Furthermore, by choosing a value of N_p^* such that $N_p^* \Delta t$ is larger than the reaction time of the control system (data acquisition, online calculation of the control forces and so on), it is possible to avoid any instability caused by time-delay effects.

Substituting Equation (12) into Equation (10):

$$\mathbf{v}[k+1] = (\bar{\mathbf{A}} + \bar{\mathbf{B}}_c \mathbf{G}_0 \mathbf{L}_0)\mathbf{v}[k] + \bar{\mathbf{B}}\mathbf{w}[k] + \bar{\mathbf{B}}_c \sum_{p=1}^{N_p} \mathbf{G}_p \mathbf{z}[k - p] + \bar{\mathbf{B}}_c \mathbf{G}_0 \mathbf{n}[k] \tag{13}$$

Now define an augmented vector $\mathbf{U}_{N_p}[k]$ as follows:

$$\mathbf{U}_{N_p}[k] \equiv [\mathbf{v}[k]^{\mathrm{T}}, \mathbf{z}[k-1]^{\mathrm{T}}, \ldots, \mathbf{z}[k - N_p]^{\mathrm{T}}]^{\mathrm{T}} \tag{14}$$

Then, Equation (13) can be rewritten as a discrete state equation for $\mathbf{U}_{N_p}$:

$$\mathbf{U}_{N_p}[k+1] = (\bar{\mathbf{A}}_u + \bar{\mathbf{B}}_{uc})\mathbf{U}_{N_p}[k] + \bar{\mathbf{B}}_u \bar{\mathbf{f}}[k] \tag{15}$$

where

$$\bar{\mathbf{f}}[k] \equiv [\mathbf{w}[k]^{\mathrm{T}}, \mathbf{n}[k]^{\mathrm{T}}]^{\mathrm{T}} \tag{16}$$

and $\bar{\mathbf{A}}_u, \bar{\mathbf{B}}_u$ and $\bar{\mathbf{B}}_{uc}$ are given by

$$\bar{\mathbf{A}}_u \equiv \begin{bmatrix} \bar{\mathbf{A}} & \mathbf{0}_{(N_{wf}+2N_d+N_{yf})\times N_p N_o} \\ \mathbf{L}_0 & \mathbf{0}_{N_o \times N_p N_o} \\ \mathbf{0}_{(N_p-1)N_o \times (N_{wf}+2N_d+N_{yf})} & \mathbf{I}_{(N_p-1)N_o}\ \mathbf{0}_{(N_p-1)N_o \times N_o} \end{bmatrix} \tag{17}$$

$$\bar{\mathbf{B}}_{uc} \equiv \begin{bmatrix} \bar{\mathbf{B}}_c \mathbf{G}_0 \mathbf{L}_0 & \bar{\mathbf{B}}_c \mathbf{G}_1 & \cdots & \bar{\mathbf{B}}_c \mathbf{G}_{N_p} \\ \mathbf{0}_{N_p N_o \times (N_{wf}+2N_d+N_{yf}+N_p N_o)} \end{bmatrix} \tag{18}$$

$$\bar{\mathbf{B}}_u \equiv \begin{bmatrix} \bar{\mathbf{B}} & \bar{\mathbf{B}}_c \mathbf{G}_0 \\ \mathbf{0}_{N_o \times N_w} & \mathbf{I}_{N_o} \\ \mathbf{0}_{(N_p-1)N_o \times N_w} & \mathbf{0}_{(N_p-1)N_o \times N_o} \end{bmatrix} \tag{19}$$

Therefore, the covariance matrix $\mathbf{\Sigma}_u \equiv E[\mathbf{U}_{N_p}[k]\mathbf{U}_{N_p}[k]^{\mathrm{T}}]$ of the augmented vector $\mathbf{U}_{N_p}$ is readily obtained:

$$\mathbf{\Sigma}_u = (\bar{\mathbf{A}}_u + \bar{\mathbf{B}}_{uc})\mathbf{\Sigma}_u(\bar{\mathbf{A}}_u + \bar{\mathbf{B}}_{uc})^{\mathrm{T}} + \bar{\mathbf{B}}_u\mathbf{\Sigma}_{\mathrm{f}}\bar{\mathbf{B}}_u^{\mathrm{T}}$$
$$\mathbf{\Sigma}_{\mathrm{f}} = \begin{bmatrix} \mathbf{\Sigma}_{\mathrm{w}} & \mathbf{\Sigma}_{\mathrm{w}n} \\ \mathbf{\Sigma}_{\mathrm{w}n}^{\mathrm{T}} & \mathbf{\Sigma}_n \end{bmatrix} \tag{20}$$

where $\mathbf{\Sigma}_f$ denotes the covariance matrix of the vector $\bar{\mathbf{f}}$ in Equation (16). Note that Equation (20) is a standard stationary Lyapunov covariance equation in discrete form.

In summary, the original continuous-time excitation, structure, actuator and output equations are transformed to a linear discrete-time state-space equation for an augmented vector $\mathbf{U}_{N_p}$. The system response is a stationary Gaussian process with zero mean and covariance matrix that can be readily calculated using Equation (20). These properties are used to design the optimal robust controller for the structure by choosing the optimal gain matrices in Equation (12) according to a suitable performance criterion.

3. OPTIMAL CONTROLLER DESIGN

The optimal robust controller is defined here as the one which maximizes the robust reliability [18] with respect to the feedback gain matrices in Equation (12), that is, the one which minimizes the robust failure probability for a structural model with uncertain parameters representing the real structural system. Failure is defined as the situation in which at least one of the performance quantities (structural response or control force) exceeds a given threshold level. This is the classic 'first passage problem', which has no closed form solution [21]. Therefore, the proposed method uses an approximate solution based on Rice's 'out-crossing' theory [21].

3.1. Conditional failure probability

Use $\mathbf{q}[k] \in \mathbb{R}^{N_q}$ to denote the control performance vector of the system at time $k\Delta t$. Its components may be structural interstorey drifts, floor accelerations, control force, etc. The system performance vector is given by

$$\mathbf{q}[k] = \mathbf{P}_0\mathbf{v}[k] + \mathbf{m}[k] \tag{21}$$

where $\mathbf{P}_0 \in \mathbb{R}^{N_q \times (N_{wf} + 2N_d + N_{yf})}$ is a performance matrix which multiplies the full state vector $\mathbf{v}$ to give the corresponding performance vector of the model. In order to account for the unmodelled dynamics, the uncertain prediction error $\mathbf{m} \in \mathbb{R}^{N_q}$ in Equation (21) is introduced because the goal is to control the system performance, not the model performance; it is modelled as discrete white noise with zero mean and covariance matrix $\mathbf{\Sigma}_m$.

For a given failure event $F_i = \{|q_i(t)| > \beta_i \text{ for some } t \in [0, T]\}$, the conditional failure probability $P(F_i|\boldsymbol{\theta})$ for the performance quantity q_i based on the structural model and excitation

model specified by $\boldsymbol{\theta}$ can be estimated using Rice's formula [21]:

$$P(F_i|\boldsymbol{\theta}) \approx 1 - \exp[-\nu_{\beta_i}(\boldsymbol{\theta})T] \tag{22}$$

where $\nu_{\beta_i}(\boldsymbol{\theta})$ is the mean out-crossing rate for the threshold level β_i and is given by

$$\nu_{\beta_i}(\boldsymbol{\theta}) = \frac{\sigma_{\dot{q}_i}}{\pi\sigma_{q_i}} \exp\left(-\frac{\beta_i^2}{2\sigma_{q_i}^2}\right) \tag{23}$$

where σ_{q_i} and $\sigma_{\dot{q}_i}$ are the standard deviation for the performance quantity q_i and its derivative $\dot{q}_i$, respectively. In implementation, $\dot{q}_i$ must be included in $\mathbf{y}_f$ in Equation (4) if it is not already part of $\mathbf{y}$.

Now consider the failure event $F = \bigcup_{i=1}^{N_q} F_i$, that is, the system fails if any $|q_i|$ exceeds its threshold β_i. Since the mean out-crossing rate of the system can be approximated by: $\nu = \sum_{i=1}^{N_q} \nu_{\beta_i}$ [22], the probability of failure $P(F|\boldsymbol{\theta})$ of the controlled structural system is given approximately by

$$P(F|\boldsymbol{\theta}) \approx 1 - \exp\left[-\sum_{i=1}^{N_q} \nu_{\beta_i}(\boldsymbol{\theta})T\right] \tag{24}$$

where N_q denotes the number of performance quantities considered.

3.2. Robust failure probability

No matter what technique (e.g. finite-element method or system identification) is used to develop a model for a structural system, the structural parameters are always uncertain to some extent. Furthermore, the excitation model is uncertain as well. Therefore, a probabilistic description is used to describe the uncertainty in the model parameters $\boldsymbol{\theta}$ defined earlier. Such probability distributions can be specified using engineering judgement or they can be obtained using Bayesian system identification techniques. This leads to the concept of the robust failure probability given by the theorem of total probability [18]:

$$P(F|\boldsymbol{\Theta}) = \int_{\boldsymbol{\Theta}} P(F|\boldsymbol{\theta})\, p(\boldsymbol{\theta}|\boldsymbol{\Theta})\, \mathrm{d}\boldsymbol{\theta} \tag{25}$$

which accounts for modeling uncertainties in deriving the failure probability. This robust failure probability is conditional on the probabilistic description of the parameters which is specified over the set of possible models $\boldsymbol{\Theta}$. Note that this high dimensional integral is difficult to evaluate numerically, so an asymptotic expansion is used [12]. Denote the integral of interest by I:

$$I = \int_{\boldsymbol{\Theta}} \mathrm{e}^{l(\boldsymbol{\theta})}\, \mathrm{d}\boldsymbol{\theta} \tag{26}$$

where $l(\boldsymbol{\theta})$ is given by

$$l(\boldsymbol{\theta}) = \ln[P(F|\boldsymbol{\theta})] + \ln[\, p(\boldsymbol{\theta}|\boldsymbol{\Theta})] \tag{27}$$

The basic idea here is to fit a Gaussian density centred at the 'design point' at which $e^{l(\boldsymbol{\theta})}$, or $l(\boldsymbol{\theta})$, is maximized. It is assumed here that there is a unique design point; see Reference [23] for a more general case. Then, this integral is approximated by

$$I \equiv P(F|\boldsymbol{\Theta}) \approx (2\pi)^{N_q/2} \frac{P(F|\boldsymbol{\theta}^*)\, p(\boldsymbol{\theta}^*|\boldsymbol{\Theta})}{\sqrt{\det \mathbf{L}(\boldsymbol{\theta}^*)}} \tag{28}$$

where $\boldsymbol{\theta}^*$ is the design point at which $l(\boldsymbol{\theta})$ has a maximum value and $\mathbf{L}(\boldsymbol{\theta}^*)$ is the Hessian of $-l(\boldsymbol{\theta})$ evaluated at $\boldsymbol{\theta}^*$. The optimization of $l(\boldsymbol{\theta})$ to find $\boldsymbol{\theta}^*$ can be performed, for example, by using MATLAB subroutine 'fmins' [24].

The proposed control design can be summarized as follows: by solving Equation (20), the covariance matrix of the structural response can be obtained. Then, the robust failure probability can be calculated using the asymptotic expansion formula in Equation (28) along with Equations (23) and (24). The optimal robust controller is obtained by minimizing the robust failure probability over all possible controllers parameterized by their gain matrices, which again can be performed, for example, using MATLAB subroutine 'fmins' [24].

The optimal controller can be readily updated when dynamic data $\mathscr{D}$ is available from the systems [5, 18, 25–28]. In this case, Bayes' Theorem is used to get an updated PDF $p(\boldsymbol{\theta}|\mathscr{D}, \boldsymbol{\Theta})$ that replaces $p(\boldsymbol{\theta}|\boldsymbol{\Theta})$ in Equation (25) and hence the updated robust failure probability $P(F|\mathscr{D}, \boldsymbol{\Theta})$ [18] is minimized to obtain the optimal control gains.

4. ILLUSTRATIVE EXAMPLES

4.1. Example 1: Four-storey building under seismic excitation

The first example refers to a four-storey building under seismic excitation with an active mass driver and a sensor on each floor above the ground level. In this example, the stochastic ground motion model is fixed during the controller design but the shear-building model of the structure (Figure 1) is uncertain. The nominal model of the structure has a floor mass and interstorey stiffness uniformly distributed over its height. The stiffness-to-mass ratios k_i/M_i, $i = 1, \ldots, 4$ is $1309.3\ \mathrm{s}^{-2}$, where M_i is the mass of floor i. The nominal damping-to-mass ratios c_i/M_i, $i = 1, \ldots, 4$ are all chosen to be equal to $2.0\,\mathrm{s}^{-1}$. As a result, the nominal modal frequencies of the uncontrolled structure are 2.00, 5.76, 8.82 and 10.82 Hz and the nominal damping ratio of the first mode is 1.00%. In order to take into account the uncertainty in the structural model parameters, all the stiffness and damping parameters are assumed to be Gaussian distributed, truncated for positive values of the stiffness and damping, with mean at their nominal values and coefficients of variation 5% (stiffness) and 20% (damping), respectively. To provide more realism, the structure to be controlled is defined by model parameters sampled from the aforementioned probability distributions rather than being equal to the nominal structural model. This gave stiffness-to-mass ratios of 1253, 1177, 1304 and $1344\ \mathrm{s}^{-2}$ for the 1st to 4th floor, respectively. The corresponding damping-to-mass ratios are 2.50, 2.16, 1.68 and $2.22\ \mathrm{s}^{-1}$.

The ratio μ of the actuator mass M_s to the total structure mass $M_o = \sum_{i=1}^{4} M_i$ is chosen to be 1%. The natural frequency ω_s and the damping ratio ζ_s of the actuator are chosen

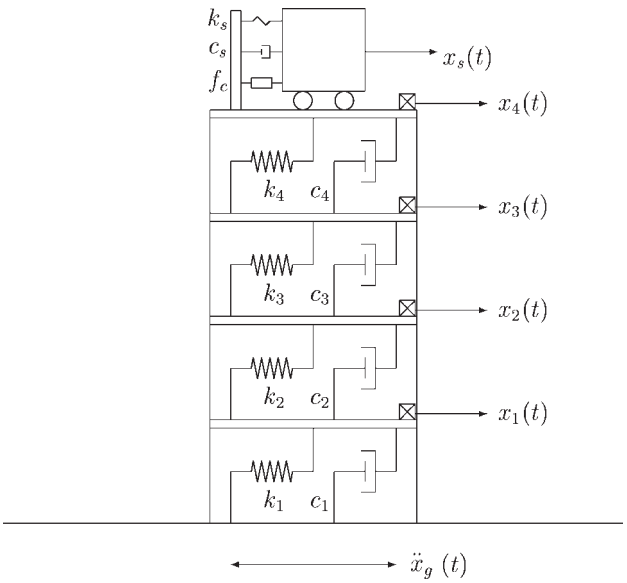

Figure 1. Four-storey shear building with active mass driver on the roof (Example 1).

according to the following expressions which give the optimal passive control system for the first mode of the nominal structure under white-noise excitation [29]:

$$\omega_s = \omega_1 \sqrt{\frac{2-\mu}{2(\mu+1)^2}}$$
$$\zeta_s = \sqrt{\frac{\mu(3\mu+4)}{2(\mu+1)(\mu+2)}} \tag{29}$$

where ω_1 is the fundamental frequency of the nominal uncontrolled structure. Then, the stiffness-to-mass ratio k_s/M_s and the damping-to-mass ratio c_s/M_s of the actuator are given by: $k_s/M_s = k_s/\mu M_o = \omega_s^2$ and $c_s/M_s = c_s/\mu M_o = 2\zeta_s\omega_s$. In this example, $k_s/M_s = 1.540 \times 10^2\ \mathrm{s}^{-2}$ and $c_s/M_s = 2.473\ \mathrm{s}^{-1}$ are the optimal parameters based on Equation (29). However, they are assumed to be, $k_s/M_s = 1.6 \times 10^2\ \mathrm{s}^{-2}$ and $c_s/M_s = 2.0\ \mathrm{s}^{-1}$ in the following since it might not be possible to build a controller with the optimal values of k_s/M_s and c_s/M_s in reality; these parameters are assumed to be known during the controller design.

The controller design is based on maximizing the robust reliability or, equivalently, minimizing the robust failure probability, calculated for the structure with uncertain parameters subject to an uncertain white-noise ground excitation with spectral intensity of $0.01\ \mathrm{m}^2\ \mathrm{s}^{-3}$ for a 20 s interval. The threshold level for the interstorey drifts, actuator stroke and the control force $f_{cn} = f_c/M_s$ (normalized by the actuator active mass) are chosen to be 2.0 cm, 2.0 m and 10 g, respectively. The failure event F of interest is the exceedance of any one of these threshold levels. For simplicity, it is assumed that displacements are measured at specified floors using a sampling interval $\Delta t = 0.01$ s. In the next example, acceleration measurements will be assumed.

Table I. Gain coefficients of the optimal controllers (Example 1).

Gain	Controller 1	Controller 2	Controller 3	Controller 4
$G_0(1)$	14.08	—	—	—
$G_0(2)$	11.87	—	—	—
$G_0(3)$	49.46	—	—	—
$G_0(4)$	32.66	86.15	134.58	—
$G_1(4)$	—	—	−26.63	237.45
$G_2(4)$	—	—	−20.98	−150.72

Table II. Robust failure probability (Example 1).

	Passive	Controller 1	Controller 2	Controller 3	Controller 4
$P(F\|\boldsymbol{\Theta})$	0.56	0.0013	0.0014	0.0008	0.0009

Four robust controllers are designed using the proposed methodology, each using different control feedback:

Controller 1: Displacement measurements at every floor at the current time step.
Controller 2: Displacement measurements at the 4th floor at the current time step.
Controller 3: Displacement measurements at the 4th floor at the current and previous two time steps.
Controller 4: Displacement measurements at the 4th floor at the previous two time steps.

Table I shows the optimal gain parameters $G_p(i)$ for Controllers 1–4 where index p and index i correspond to the number of time-delay steps and the floor number, respectively. Table II shows the robust failure probability for passive control (all gain coefficients are fixed at zero) and for Controllers 1–4. The active controllers give a much better design performance objective than the passive mass damper. All controllers give similar design performance objectives but Controller 3 is the best, followed by Controllers 4 and 1, and then 2. Although the number of measured degrees of freedom is different in Controllers 1 and 2, the performance of the controlled structure is almost the same. This is because the motion of the structure is dominated by the first mode in the case of ground shaking. Therefore, the measurements at one DOF contain almost all of the information regarding the motion of the structure. However, Controller 3 gives a better performance objective than Controller 1 even though Controller 3 uses only one sensor because measuring displacements at consecutive time steps gives more information.

Figures 2–5 show the time histories of the interstorey drifts under the design excitation for Controllers 1–4, respectively. The dashed and solid curves show the response of the uncontrolled and controlled structure, respectively, during simulated operation under the same ground motion sampled from the stochastic ground motion model. It can be seen that the interstorey drifts are significantly reduced by the controllers. Furthermore, Table III shows the statistical properties (standard deviations and maximum) of the performance quantities (interstorey drifts, actuator stroke and actuator acceleration) for the uncontrolled structure, passive control and Controllers 1–4. By comparing Controllers 1 and 2 in Table II, one

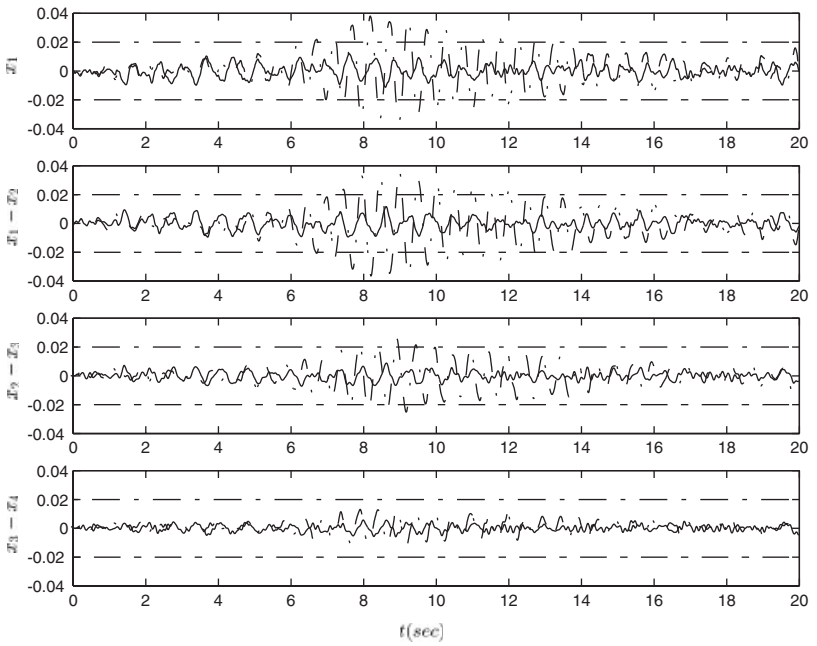

Figure 2. Simulated interstorey drifts (in metres) for the uncontrolled (dashed) and controlled structure using Controller 1 (solid) (Example 1).

observes that the robust failure probabilities are very similar. Furthermore, Table III shows that the performance quantities in these two cases are almost the same. This implies that the performance when using feedback from one or four (all) degrees of freedom are virtually the same. As mentioned before, this is because the motion of the structure is dominated by the first mode in the case of ground shaking and so using the measurements at one degree of freedom is sufficient to characterize the motion of the structure. Note that although Controller 3 gives the smallest probability of failure in Table II, the performance quantities in Table III are almost the same for all optimal controllers.

Controller 4 is the case in which the controller feeds back the measurements at past time steps only. Although its robust failure probability is slightly larger than Controller 3 in Table II, the performance quantities in Table III are virtually the same as Controller 3. Moreover, this controller does not suffer from any stability problem induced by any time delays if the time-delay of the controller Δt_{d} is less than Δt. If Δt_{d} is larger than Δt, one can choose $N_p > \Delta t_{\mathrm{d}}/\Delta t$ and fix all the matrices $\mathbf{G}_0, \ldots, \mathbf{G}_{\mathrm{INT}}(\Delta t_{\mathrm{d}}/\Delta t)$ at zero. Here, INT denotes the integer part of a number. Then, the controller uses the measurements far back enough in time that the control system has enough time to compute and apply the control command. Figures 6 and 7 show the similar control force (normalized by the actuator mass) and stroke time histories respectively for Controllers 1–4.

In order to test the robustness of the proposed controller to the excitation, the structural response is calculated for the uncontrolled structure and the controlled structure (using Controller 3) subjected to the 1940 El Centro earthquake record. In Figure 8, the dashed line and the solid line show the first storey drifts for the uncontrolled structure and the controlled

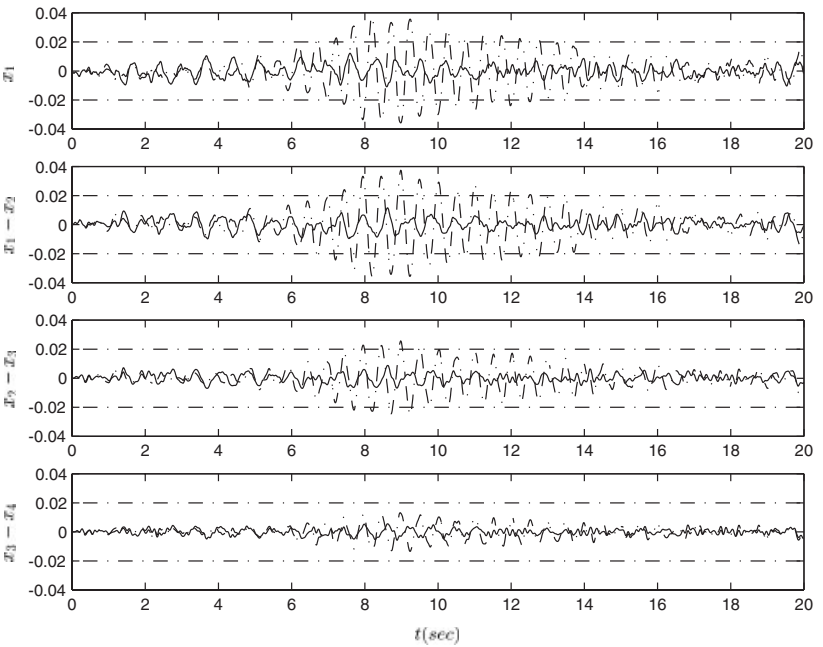

Figure 3. Simulated interstorey drifts (in metres) for the uncontrolled (dashed) and controlled structure using Controller 2 (solid) (Example 1).

structure, respectively. It can be seen that the structural response is significantly reduced by using the proposed controller. In this case, the peak control force normalized by the actuator mass is 1.7 g and the peak actuator stroke is 0.23 m.

4.2. Example 2: Control benchmark problem

The proposed control strategy is applied to the well-known control benchmark problem with an active mass driver [30]. The benchmark problem is based on a three-storey, single-bay laboratory test structure [31]. It is a steel frame of height 158 cm. The natural frequencies of the first three modes are 5.81, 17.68 and 28.53 Hz, respectively. The associated damping ratios are 0.33, 0.23 and 0.30%. In this example, the structural system is assumed known (an accurate dynamic model is given in the benchmark, but the stochastic excitation model is treated as uncertain). The controllers are designed and tested under the excitation of a Kanai–Tajimi filtered white noise, and further tested using a scaled 1940 El Centro earthquake record and a scaled 1968 Hachinohe earthquake record. The sampling time intervals is $\Delta t = 0.001$ s, as specified by the benchmark. The threshold levels for the interstorey drifts, actuator displacements and actuator accelerations are 1.5 cm, 9.0 cm and $6.0g$, respectively. As the delay time of the control force is $\Delta t_{\mathrm{d}} = 0.0002$ s, the controllers in this study are chosen to feedback only the response measurements from one and two time steps back, that is, $\mathbf{G}_0$ is fixed to be zero and $\mathbf{G}_i$, $i = 1, 2$ are the design parameters. Two feedback cases were investigated as follows:

Controller 1: Feedback of acceleration from all floors at the previous two time steps, i.e. $\mathbf{G}_i$, $i = 1, 2$ are the design parameters.

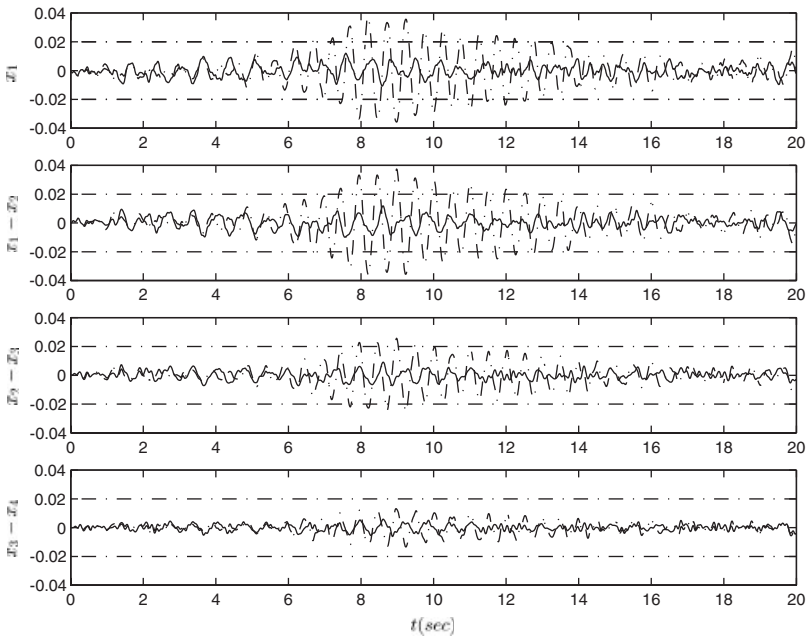

Figure 4. Simulated interstorey drifts (in metres) for the uncontrolled (dashed) and controlled structure using Controller 3 (solid) (Example 1).

Controller 2: Acceleration measurements from all floors are passed through the same low-pass filter with transfer function $\omega_c^2/(-\omega^2 + 2i\zeta_c\omega_c\omega + \omega_c^2)$. Then, the controller feeds back the filtered measurements at the previous two time steps. Here, ζ_c is chosen to be $1/\sqrt{2}$ and ω_c is included in the design parameter set. This case has been previously studied using only output of the filter at the current time [14].

Following the benchmark guidelines [30], the controllers are used to control a high-fidelity linear time-invariant state-space representation of the structure which has 28 states. Quantization, saturation and time delay of the control force are considered in this model. In order to test the robustness of the controllers with respect to modeling errors, a reduced 10-state model is used in the design process, which is provided at the official benchmark web site at http://www.nd.edu/∼quake/. Furthermore, the excitation is assumed to be a stationary zero-mean Gaussian process with a spectral density defined by an uncertain Kanai–Tajimi spectrum:

$$S_{\ddot{x}_g\ddot{x}_g} = S_0 \frac{4\zeta_g^2\omega_g^2\omega^2 + \omega_g^4}{(\omega^2 - \omega_g^2)^2 + 4\zeta_g^2\omega_g^2\omega^2} \tag{30}$$

where ω_g, ζ_g are assumed to be log-normally distributed with mean 50 rad/s and 0.5, respectively. Furthermore, their logarithm standard deviations are assumed to be $\sigma_{\log\,\omega_g} = 0.2$ and

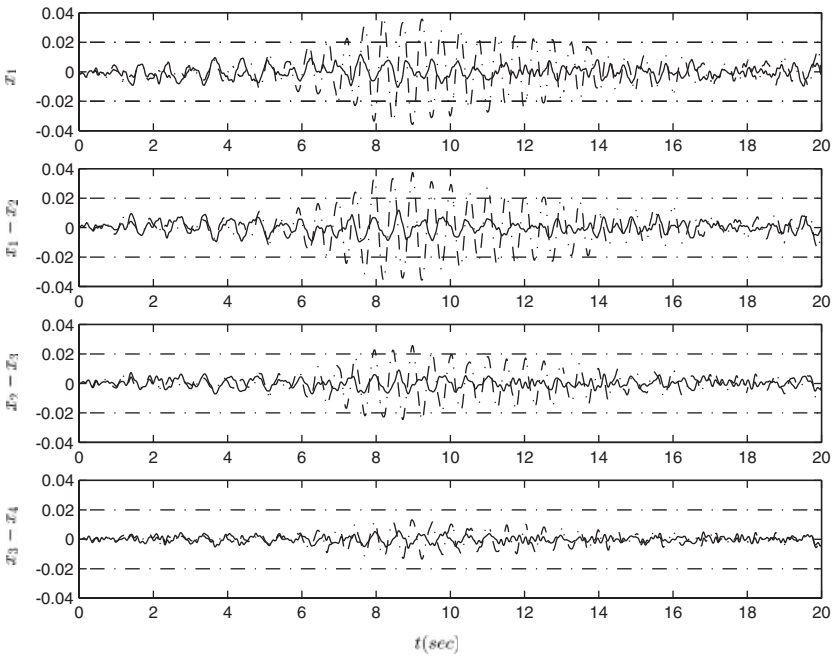

Figure 5. Simulated interstorey drifts (in metres) for the uncontrolled (dashed) and controlled structure using Controller 4 (solid) (Example 1).

Table III. Performance quantities for interstorey drifts and actuator stroke and acceleration under the design excitation (Example 1).

Performance quantity	Threshold	Uncontrolled	Passive	Controller 1	Controller 2	Controller 3	Controller 4
σ_{x_1} (m)	—	0.0143	0.0075	0.0042	0.0042	0.0040	0.0040
$\sigma_{x_1-x_2}$ (m)	—	0.0138	0.0072	0.0039	0.0039	0.0037	0.0037
$\sigma_{x_2-x_3}$ (m)	—	0.0095	0.0050	0.0029	0.0028	0.0027	0.0028
$\sigma_{x_3-x_4}$ (m)	—	0.0053	0.0029	0.0021	0.0020	0.0019	0.0020
$\max \lvert x_1 \rvert$ (m)	0.02	0.0373	0.0213	0.0120	0.0122	0.0114	0.0115
$\max \lvert x_1 - x_2 \rvert$ (m)	0.02	0.0374	0.0197	0.0117	0.0116	0.0113	0.0114
$\max \lvert x_2 - x_3 \rvert$ (m)	0.02	0.0257	0.0143	0.0088	0.0088	0.0086	0.0087
$\max \lvert x_3 - x_4 \rvert$ (m)	0.02	0.0134	0.0085	0.0059	0.0058	0.0059	0.0060
σ_{x_s} (m)	—	—	0.1019	0.4056	0.3934	0.4101	0.4071
$\sigma_{f_{cn}}$ (g)	—	—	—	2.7764	2.6656	2.7785	2.7905
$\max \lvert x_s \rvert$ (m)	2.0	—	0.2984	1.0756	1.0374	1.0897	1.0895
$\max \lvert f_{cn} \rvert$ (g)	10.0	—	—	8.0942	7.9589	8.3669	8.509

$\sigma_{\log \zeta_g} = 0.2$. The spectral intensity parameter S_0 is given by

$$S_0 = \frac{0.03\zeta_g}{\pi\omega_g(4\zeta_g^2 + 1)} \, \mathrm{g^2 s} \tag{31}$$

such that $\sigma_{\ddot{x}_g} = 0.12\,g$ regardless of the values of ω_g and ζ_g.

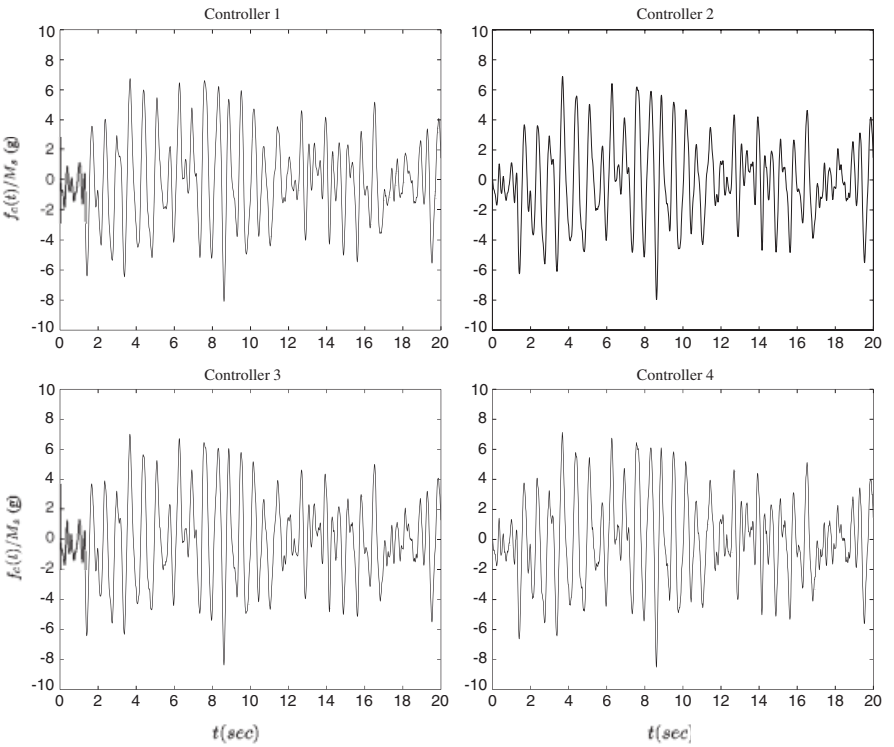

Figure 6. Controller force (normalized by the actuator mass) time histories using Controllers 1–4 (Example 1).

Table IV shows the optimal gains and the optimal filter frequency parameter for Controllers 1 and 2. One can see that the control gains increase significantly when using the low-pass filter. Table V shows the performance quantities J_1 to J_{10} defined in Reference [30] for Controllers 1 and 2, for the controller obtained by May and Beck [14] and also for the sample controller provided in Reference [30]. All the controllers provide satisfactory performance. Note that the controller obtained by May and Beck is similar to Controller 2 except that they only feed back the response measurements at the current time. Their optimal gains are $G_0(1) = 0.431$, $G_0(2) = 0.291$, and $G_0(3) = 0.235$ and their optimal filter frequency parameter is $\omega_c = 33.1$ rad/s. J_1 to J_5 correspond to the case of uncertain excitation for 300 s. J_1 and J_2 correspond to the standard deviations of the maximum RMS drifts and the maximum RMS absolute acceleration of the controlled structure over all of the floors, normalized by the corresponding values for the uncontrolled structure. J_3, J_4 and J_5 correspond to the RMS actuator displacement relative to the third storey, the RMS relative actuator velocity and the RMS absolute actuator acceleration. Again, they are normalized by their corresponding values for the uncontrolled structure. J_6–J_{10} represent the peak values of the same response quantities for the deterministic response of the controlled structure to the two scaled earthquake ground motions, the north–south component of the 1940 El Centro earthquake record and the north–south component of the 1968 Hachinohe earthquake record. Again, these quantities

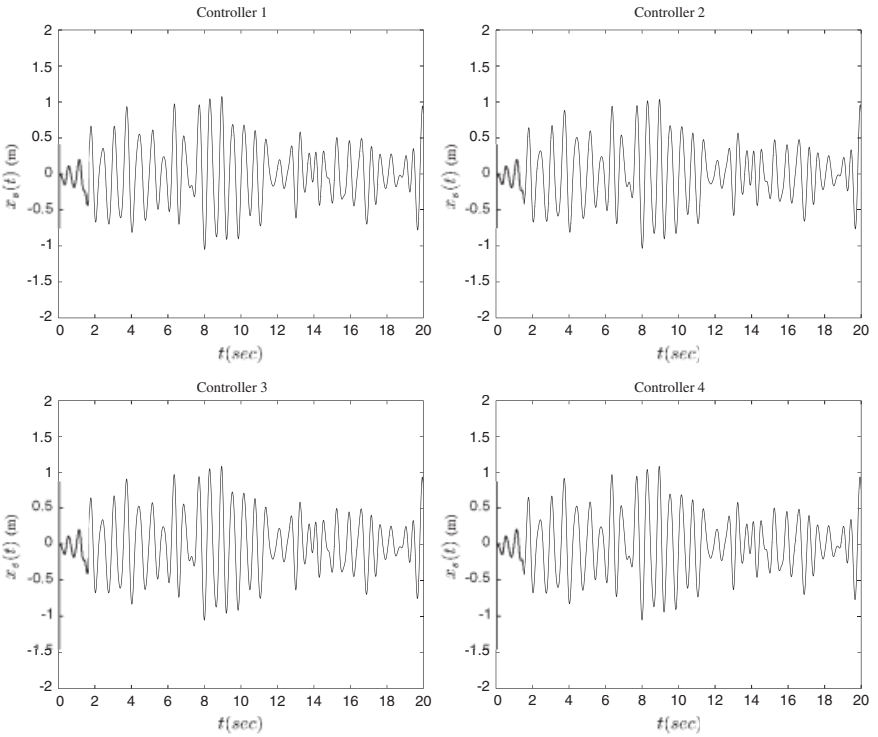

Figure 7. Controller stroke time histories (in metres) using Controllers 1–4 (Example 1).

are normalized by the peak response quantities of the uncontrolled structure for each earthquake.

Previous work [14] showed that directly feeding back the accelerations at the current time without a compensator leads to an unstable controlled system due to the delay-time imposed in the model of the system to be controlled [30]. However, Controller 1 provides satisfactory performance using direct feedback of delayed accelerations because the delay-time is explicitly taken into consideration in the formulation, as described in Section 2. In Reference [14], a filter was used in the feedback loop to produce stability. When a filter is used here (Controller 2), the control system is not as efficient as in Controller 1 when subjected to random excitation because certain information, especially the high frequency content, is filtered out. However, Table V shows it provides better performance for the El Centro and the Hachinohe earthquake records, which do not follow the Kanai–Tajimi spectrum closely.

Figure 9 shows the first storey drift for both earthquakes using Controller 2 (solid curve) which has the low-pass filter. For comparison purposes, the dashed lines show the corresponding first storey drifts of the uncontrolled structure. It can be seen that these drifts are significantly reduced by using the proposed control methodology. Figure 10 shows the actuator displacements for both earthquakes. It can be seen that they are much smaller than the threshold values.

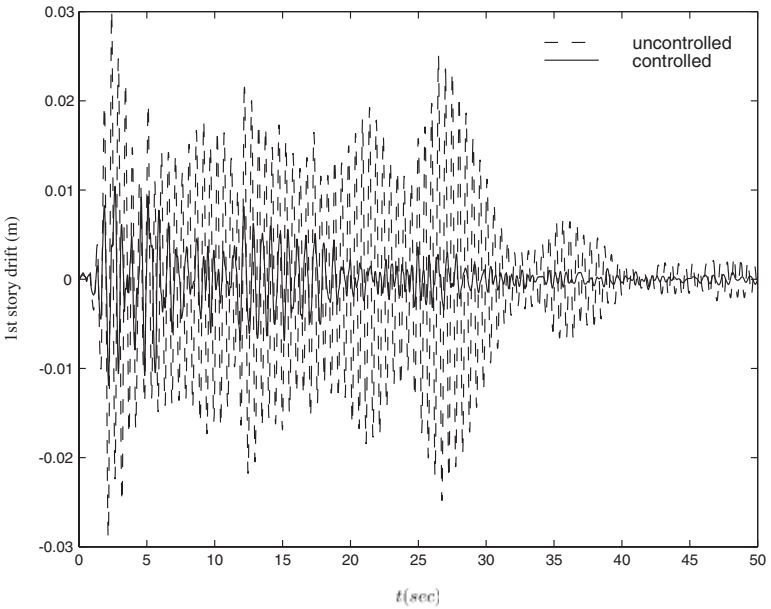

Figure 8. First storey drift (in metres) of the uncontrolled (dashed) and controlled structure using Controller 3 (solid) to the El Centro earthquake record (Example 1).

Table IV. Design parameters for the optimal controllers (Example 2).

Gain\Controller	1	2
$G_1(1)$	0.0062	0.0930
$G_1(2)$	0.0014	0.0959
$G_1(3)$	0.0228	0.0931
$G_2(1)$	0.0319	0.1268
$G_2(2)$	0.0494	0.1056
$G_2(3)$	0.0838	0.1047
ω_c(rad/s)	—	44.993

5. CONCLUDING REMARKS

A reliability-based robust feedback control approach was presented for dynamical systems adequately represented by linear state space models. The response covariance matrix is first obtained from the discrete Lyapunov equation using an augmented vector for the system. The optimal controller is then chosen from a set of possible controllers so that the robust reliability of the controlled system is maximized or, equivalently, the robust failure probability is minimized. An asymptotic approximation is used to evaluate the high-dimensional integrals for the robust failure probability. The feedback of the past output provides additional information about the system dynamics to the controller. It can also be used to avoid stability

Table V. Performance quantities for the benchmark problem (Example 2).

Excitation	Performance quantity	Controller 1	Controller 2	May and Beck [14]	Sample controller [30]
Filtered white noise	J_1	0.183	0.205	0.207	0.283
	J_2	0.301	0.310	0.345	0.440
	J_3	0.366	0.736	0.851	0.510
	J_4	0.363	0.738	0.832	0.513
	J_5	0.606	0.676	0.683	0.628
Maximum response of Hachinohe 1968 and El Centro 1940	J_6	0.492	0.380	0.380	0.456
	J_7	0.811	0.694	0.684	0.681
	J_8	0.812	1.39	1.64	0.669
	J_9	0.847	1.35	1.56	0.771
	J_{10}	1.64	1.16	0.936	1.28

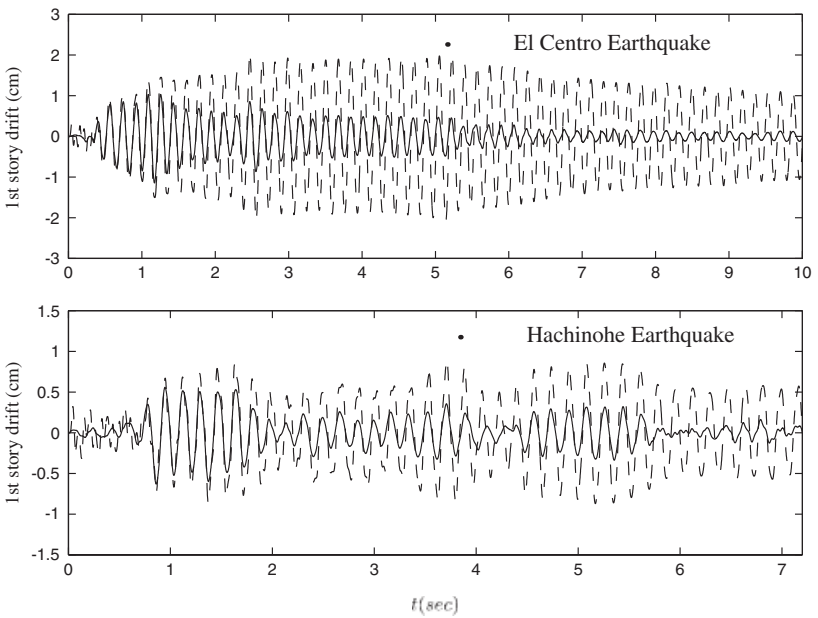

Figure 9. First storey drift (in cm) of the uncontrolled (dashed) and controlled structure using Controller 2 (solid) to the El Centro and Hachinohe earthquake records (Example 2).

problems due to time-delay effects. The proposed approach does not require full state measurements or a Kalman filter to estimate the full state. The robust failure probability criterion provides robustness of the control for both uncertain excitation models and uncertain system models. Furthermore, it can give different weighting to the different possible values of the model parameters by using a probability description of these parameters based on engineering judgement or obtained from system identification techniques. This is in contrast to most

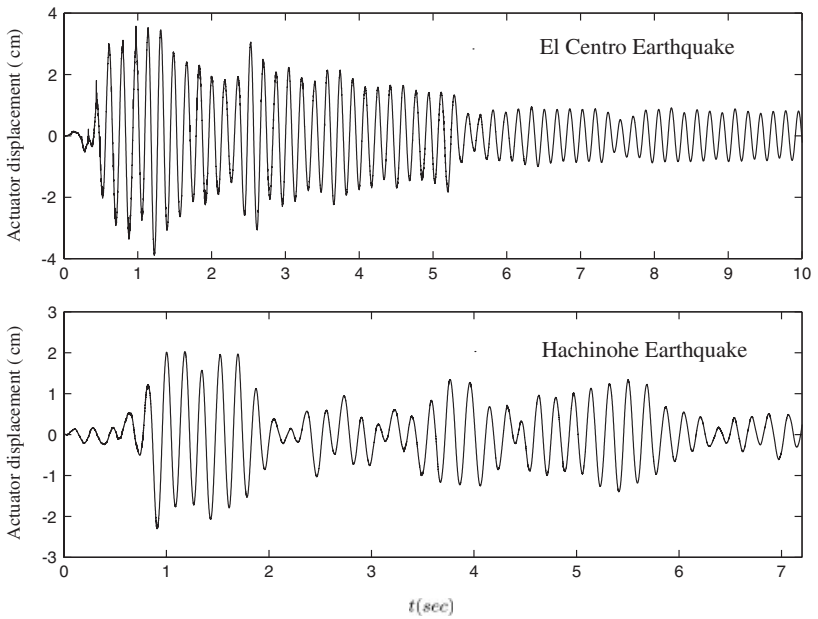

Figure 10. Actuator displacement (in cm) using Controller 2 to the El Centro and Hachinohe earthquake records (Example 2).

current robust control methods which split the values for the system parameters into only two groups (possible or impossible).

REFERENCES

1. Doyle JC, Glover K, Khargonekar PP, Francis BA. State-space solutions to standard $\mathscr{H}_2$ and $\mathscr{H}_\infty$ control problems. *IEEE Transactions on Automatic Control* 1989; **34**(8):831–847.
2. Doyle JC, Francis BA, Tannenbaum AR. *Feedback Control Theory*. Macmillan: UK, 1992.
3. Cox RT. *The Algebra of Probable Inference*. Johns Hopkins Press: Baltimore, 1961.
4. Beck JL. System identification methods applied to measured seismic response. In *Proceedings of Eleventh World Conference on Earthquake Engineering*. Elsevier: New York, 1996.
5. Beck JL, Katafygiotis LS. Updating models and their uncertainties. I: Bayesian statistical framework. *Journal of Engineering Mechanics* (ASCE) 1998; **124**(4):455–461.
6. Stengel RF, Ray LR. Stochastic robustness of linear time-invariant control systems. *IEEE Transactions on Automatic Control* 1991; **36**(1):82–87.
7. Marrison CI, Stengel RF. Stochastic robustness synthesis applied to a benchmark problem. *International Journal of Robust Nonlinear Control* 1995; **5**:13–31.
8. Spencer BF, Kaspari DC. Structural control design: a reliability-based approach. In *Proceedings of American Control Conference*, Baltimore, MD, 1994; 1062–1066.
9. Spencer BF, Kaspari DC, Sain MK. Reliability-based optimal structural control. In *Proceedings of Fifth U.S. National Conference on Earthquake Engineering*, EERI, Oakland, California, 1994; 703–712.
10. Field RV, Hall WB, Bergman LA. A MATLAB-based approach to the computation of probabilistic stability measures for controlled systems. In *Proceedings of First World Conference on Structural Control*, *International Association for Structural Control*, Pasadena, 1994; TP4-13–TP4-22.
11. Field RV, Voulgaris PG, Bergman LA. Probabilistic stability robustness of structural systems. *Journal of Engineering Mechanics* (ASCE) 1996; **122**(10):1012–1021.
12. Papadimitriou C, Beck JL, Katafygiotis LS. Asymptotic expansions for reliability and moments of uncertain systems. *Journal of Engineering Mechanics* (ASCE) 1997; **123**(12):1219–1229.

13. Papadimitriou C, Katafygiotis LS, Au SK. Effects of structural uncertainties on TMD design: A reliability-based approach. *Journal of Structural Control* 1997; **4**(1):65–88.
14. May BS, Beck JL. Probabilistic control for the active mass driver benchmark structural model. *Earthquake Engineering and Structural Dynamics* 1998; **27**(11):1331–1346.
15. Soong TT. *Active Structural Control*: *Theory and Practice*. Wiley: New York, 1990.
16. Housner GW, Bergman LA, Caughey TK, Chassiakos AG, Claus RO, Masri SF, Skelton RE, Soong TT, Spencer BF, Yao JTP. Special issue on structural control: past, present, and future. *Journal of Engineering Mechanics* (ASCE) 1997; **123**(9).
17. Caughey TK (Ed.). Special issue on benchmark problems. *Earthquake Engineering and Structural Dynamics* 1998; **27**(11):1127–1397.
18. Papadimitriou C, Beck JL, Katafygiotis LS. Updating robust reliability using structural test data. *Probabilistic Engineering Mechanics* 2001; **16**(2):103–113.
19. Dyke SJ, Spencer BF, Quast P, Sain MK. Role of control-structure interaction in protective system design. *Journal of Engineering Mechanics* (ASCE) 1995; **121**(2):322–338.
20. Ivers DE, Miller LR. *Semi-Active Suspension Technology*: *An Evolutionary View*. Advanced Automotive Technologies, ASME Book No. H00719, 1991.
21. Lin YK. *Probabilistic Theory of Structural Dynamics*. Krieger: Malabar, FL, 1976.
22. Veneziano D, Grigoriu M, Cornell CA. Vector-process models for system reliability. *Journal of Engineering Mechanics* (ASCE) 1977; **103**(EM3):441–460.
23. Au SK, Papadimitriou C, Beck JL. Reliability of uncertain dynamical systems with multiple design points. *Structural Safety* 1999; **21**:113–133.
24. MATLAB. *Matlab User's Guide*. The MathWorks, Inc.: Natick, MA, 1994.
25. Yuen K-V, Katafygiotis LS. Bayesian modal updating using complete input and incomplete response noisy measurements. *Journal of Engineering Mechanics* (ASCE) 2002; **128**(3):340–350.
26. Yuen K-V, Beck JL, Katafygiotis LS. Probabilistic approach for modal identification using non-stationary noisy response measurements only. *Earthquake Engineering and Structural Dynamics* 2002; **31**(4):1007–1023.
27. Yuen K-V, Beck JL. Updating properties of nonlinear dynamical systems with uncertain input. *Journal of Engineering Mechanics* (ASCE) 2003; **129**(1):9–20.
28. Yuen K-V. PhD thesis: Model selection, identification and robust control for dynamical systems. Technical Report EERL 2002-01, California Institute of Technology, Pasadena, USA, 2002.
29. Warburton GB, Ayorinde EO. Optimal absorber parameters for simple systems. *Earthquake Engineering and Structural Dynamics* 1980; **8**:179–217.
30. Spencer BF, Dyke SJ, Deoskar HS. Benchmark problems in structural control: Part I-Active mass driver system. *Earthquake Engineering and Structural Dynamics* 1998; **27**(11):1127–1139.
31. Dyke SJ, Spencer BF, Quast P, Kaspari DC, Sain MK. Implementation of an active mass driver using acceleration feedback control. *Microcomputers in Civil Engineering* 1996; **11**:305–323.

